OPTOELECTRONICS AND ADVANCED MATERIALS – RAPID COMMUNICATIONS Vol. 3, No. 7, July 2009, p. 655 - 658

Design of silicon optical modulator based on complete TM photonic band-gap

G. S. KLIROS*, A. N. FOTIADIS, G. P. TZIOPIS
Department of Aeronautical Sciences, Division of Electronics and Communication Engineering, Hellenic Air-Force Academy, Dekeleia Attica GR-1010, Greece

We report on the design of a novel silicon optical modulator based on photonic crystals with complete transverse-magnetic (TM) photonic band-gap (PBG). The device operation is based on a dynamic shift of the complete PBG due to induced change in the silicon refractive index by free carrier injection. The plane-wave expansion method (PWE) and finite-difference time-domain (FDTD) simulation were utilized to design the device and investigate its light modulation performance. With small size, rapid response time and high extinction ratio, the proposed optical modulator can be easily implemented to design ultra-compact all optical integrated circuits.

(Received June 11, 2009; accepted July 20, 2009)

Keywords: Optical modulator, Photonic crystal waveguides, Silicon photonics, Photonic band-gap

1. Introduction

Optical components that permit the miniaturization of specific optical integrated circuits to a scale comparable to the wavelength of light are good candidates for realizing high density photonic integrated circuits. In recent years, there has been a growing effort in the realization of active and passive photonic crystal waveguides (PhCWs) as ultra-compact optical components and circuits [1,2], which can be integrated monolithically on a single chip. The theoretical and the experimental investigations demonstrate that PhCWs can be applied to the wide-aperture single-mode lasers [3], wavelength filters [4], wavelength division multiplexing and demultiplexing devices [5, 6] as well as photonic band-gap polarizers [7].

Optical modulators are pivotal components in photonic integrated circuits. Up to now, various schemes of optical modulators have been proposed such as electro-optical material modulators [8,9] and III-V semiconductor material modulators [10]. However, electro-optical material (e.g. $LiNbO_3$) modulators are not easy to be integrated and their sizes are too long. Despite of the high performance achieved, the III-V semiconductor materials modulators have complex structures and high fabrication costs. On the other hand, as silicon photonics technology [11] is compatible with conventional CMOS processing, monolithic integration of silicon photonic devices with advanced electronics on a single silicon substrate becomes possible. Recently, some new kinds of silicon optical modulators have been proposed [12-15] where a defect waveguide based on triangular PhC is incorporated in the device leading to a reduction of the modulator electrode length by several orders of magnitude. In most designs, the modulator operation is based on plasma dispersion effects [16], through which free carrier concentration perturbation results in refractive index change. Carrier injection and capacitive coupling through MOS field effect are two major methods to introduce the free carriers into silicon. In MOS-based silicon modulator, the overlap between the optical field and carrier perturbation area is usually small because the efficient free-carrier concentration variations only presents within a thin silicon layer beneath the insulated gate region. However, in p-i-n configuration, overlap between the optical field and electrical field can be maximized, since the free carriers will be uniformly injected into a comparative large intrinsic area that covers the whole wave-guiding region. The switching speed of such a p-i-n diode-based device is usually determined by the carrier recombination time and carrier transit time [16].

In this paper, a novel silicon optical modulator based on a honeycomb photonic crystal with a complete photonic band-gap (PBG), is proposed. A horizontal p-i-n configuration is utilized where the light modulation mechanism is based on the dynamic shift of the PBG as free carriers are injected into the wave-guiding region. The PBG computations have been done using the plane-wave expansion method (PWE) and the modulator has been modelled by the finite-difference time-domain (FDTD) method.

2. Device design and simulation

The configuration of the proposed integrated PhC modulator using silicon-on-insulator (SOI) technology is shown schematically in Fig. 1. A PhC structure composed of two dimensional (2D) honeycomb pattern of holes drilled in intrinsic silicon (Si) (n = 3.4), has been selected for the design of the wave-guiding region. A line defect waveguide is formed by missing a row of air holes in the Γ-K direction. As is well known, the line defect breaks the bang-gap effect and due to high-index contrast system,

guided modes with low group velocity are supported [13]. In addition, positive and negative poles are arranged on the top of n-type and p-type silicon PhC, respectively. The choice of the honeycomb hole-lattice has been motivated by previous studies [17,18] where PhCs relying on the honeycomb lattice geometry exhibit the largest TM PBG compared to the PhCs based on square or triangular lattice geometries. As is discussed in Ref. [19], for 2D photonic crystals, TM optical band-gaps are favoured in a lattice of isolated high-ε regions. Unfortunately, this configuration is incompatible with an electrical injection device due to its non-connected nature. Furthermore, although a few more complex structures can be modelled to achieve a TM PBG by varying additional parameters (e.g., the shape or orientation of air-holes) [20,21], most of them show limited manufacturability at telecommunication wavelengths.

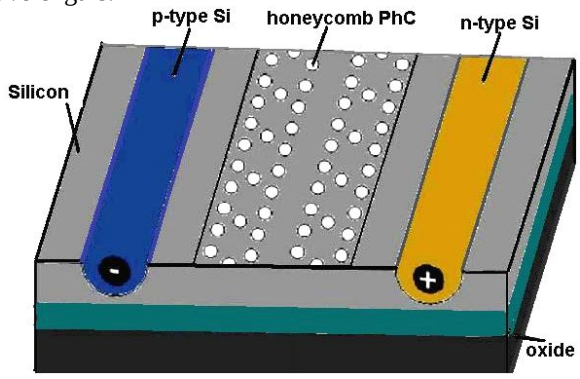

(a)

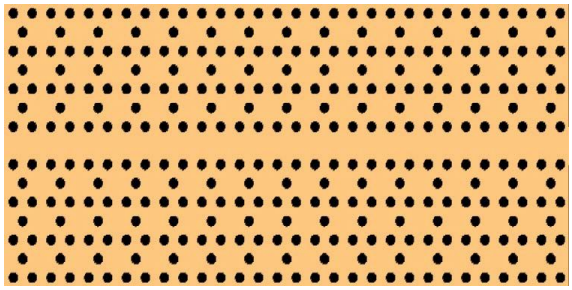

(b)

Fig. 1. (a) Schematic diagram of the silicon p-i-n modulator and (b) the embedded honeycomb-PhC structure.

In general, the control of PBG-shift depends on the geometry of the PhC and the refractive index of the dielectric materials. In this work, the refractive index change of the silicon PhC is produced by the free carrier injection. There are three mechanisms by which free carriers can induce changes to silicon refractive index. These include contributions from the Drude effect, band filling and band-gap narrowing. Here, only the Drude contribution is considered. The silicon refractive index changes depend on free carrier concentration by the dispersion relation that can be derived, in a first order approximation, by the classical Drude model [22]:

$$\Delta n = -\frac{e^2\lambda^2}{8\pi^2 c^2 \varepsilon_o n}\left(\frac{\Delta N_e}{m_e}+\frac{\Delta N_h}{m_h}\right) \qquad (1)$$

where Δn is the variation of the real part of refractive index (n) when the free carrier concentration deviates from the values of the intrinsic semiconductor, λ is the operating wavelength, c is the light speed in vacuum, ε_0 is the permittivity in free space, n is the refractive index of intrinsic silicon, ΔN is the free carrier concentration variation, and m is the effective masses. The subscripts e and h refer to electrons and holes, respectively. In this work, the refractive index of intrinsic silicon (n) is set to be 3.4. In n-type and p-type silicon zone with an electron-hole concentration of 3×10^{19} cm^{-3} at a field strength of 8×10^5 V/cm, there is a negative refractive-index change of Δn=0.1 between the depleted and undepleted regions, at the optical wavelength λ=1550 nm.

The plane wave expansion method (PWE) was utilized to generate the photonic band-gap map (Fig. 2) and PBG-diagrams for TM-polarization (Fig. 3). We select a normalized hole radius r/a=0.23 to have a maximum range of the complete PBG.

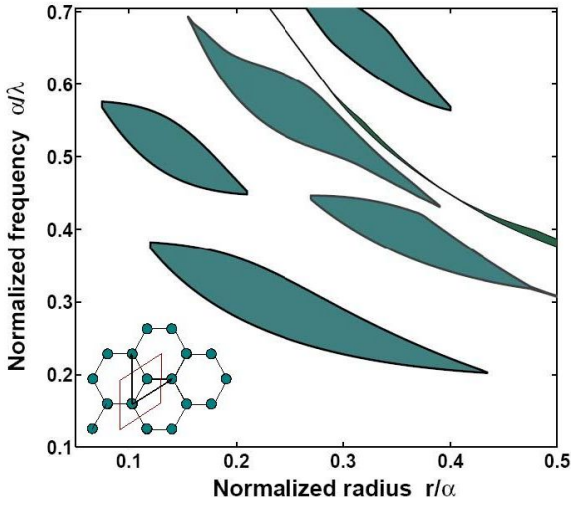

Fig. 2. The band gap map of honeycomb PhC of air holes.

Fig. 3(a) and (b) show the band diagram in the case of without and with free carrier injection, respectively. From Fig. 3(a), one sees that the band-gap normalized frequency (α/λ) range is, from 0.326 to 0.350 without free carrier injection. When the free carriers are injected, the band-gap frequency (α/λ) range is, from 0.336 to 0.360. It can be observed that the band gap shifts with the change of the silicon photonic crystal refractive index due to free carrier injection. In the following, the normalized frequency α/λ=0.335 is employed to model the transmission power of the waveguide by using two-dimensional FDTD [23]. This frequency is a guided mode in the absence of free carrier injection but it is not a guided mode for the case of carrier

injection. Since our work focused on operating wavelength λ=1550 nm, a lattice constant in the PhCW of the modulator α=520 nm, is obtained.

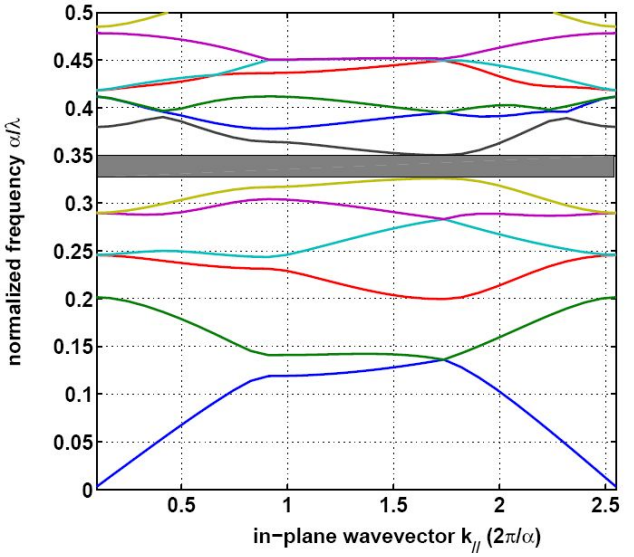

(a)

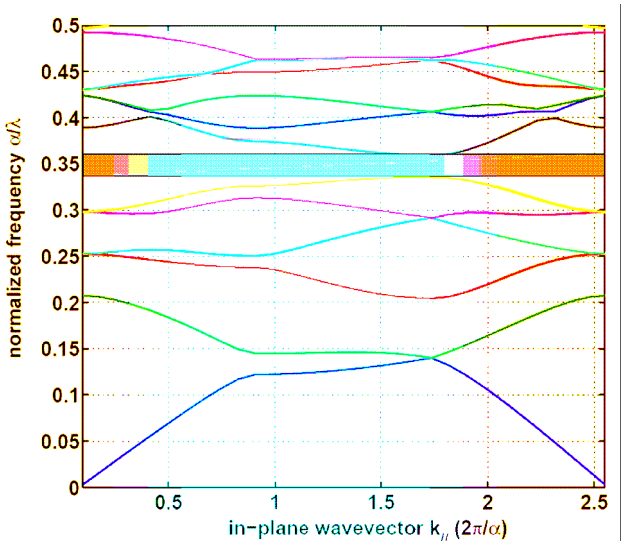

(b)

Fig. 3. TM band diagram of honeycomb PhC of air holes with radius r =0.23a drilled in a high r efractive index silicon (a) without and (b) with carrier injection.

Fig. 4 (a) and (b) show the optical power flow in the optical modulator without, and with free carrier injection, respectively. It can be observed that the light wave can propagate in the waveguide without free carrier injection. Moreover, the optical power passes the optical modulator with less transmission loss. However, the propagation in the waveguide is forbidden with free carrier injection and the optical power no longer passes the structure but instead, is nearly completely reflected. Therefore, small changes in the refractive index can cause dramatic changes in the transmitted intensity of light over very short distances. Consequently, the light intensity in the line defect PhCW can be strongly modulated by free carrier injection change in the refractive index of silicon. The size of the modulator is about 45α = 23.4 μm at λ=1.55 μm. Only a few microns (≲10 μm) of length are required to modulate the intensity of the light. The modulator exhibited a high extinction ratio in the forbidden state and a low insertion loss in the propagation state.

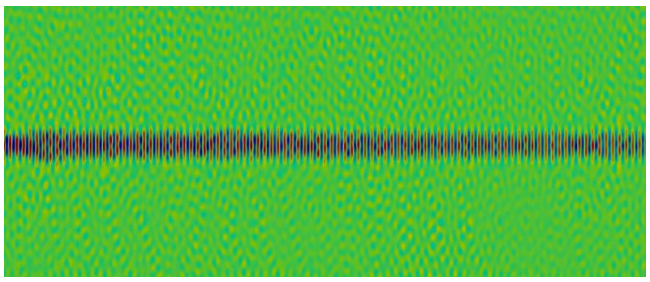

(a)

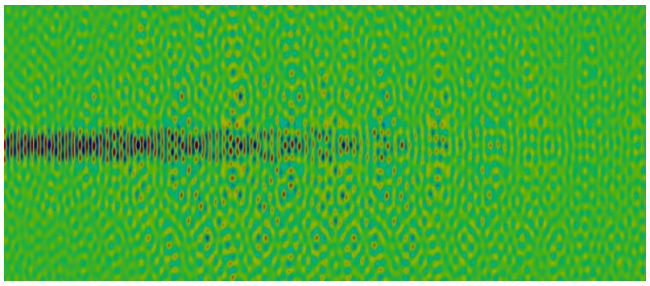

(b)

Fig. 4. FDTD simulation of the optical power flow in the designed optical modulator: (a) without and (b) with carrier injection.

3. Conclusions

We have designed and investigated a novel optical modulator with p-i-n configuration utilizing photonic crystals with complete transverse magnetic PBG. The modulation mechanism is based on dynamic PBG-shift induced by free carrier injection. The PWE method and FDTD simulation were employed in order to design the device and investigate its light modulation performance. The simulation results, at the telecommunication wavelength 1.55 μm, show that the designed optical modulator exhibits a high extinction ratio, low insertion loss, and small size. Since it is silicon-based, the proposed modulator can be easily implemented to design ultra-compact all optical integrated circuits.

References

[1] M. Notomi, NTT - Tech. Rev. **4**, 6 (2006).
[2] M. Kamp, T. Happ, S. Mahnkopf, G. Duan, S. Anand, A. Forhel, Physica E **21**, 802 (2004).
[3] N**.** Yokouchi**,** A. Y. Danner, K. D. Choquette, IEEE J. Sel. Top. Quant. Electron. **9**, 1439 (2003).
[4] Y. Akahane, T. Asano, B. Song, S. Noda, Opt. Express **13**, 1202 (2005).
[5] A. D'Orazio, M. De Sario, V. Petruzzelli, F. Prudenzano, Opt. Express **11**, 230 (2003).
[6] I. A. Sukhoivanov, I. V. Guryev, O. V. Shulika, A. V. Kublyk, O. V. Mashoshina, E. Alvaradoméndeza, J. A. Andrade-Lucioa, J. Optoel**.** Adv**.** Mater**. 8**(4), 1622 **(**2006).
[7] Y. Cui, Qi Wu, E. Schonbrun, M. Tinker J. B. Lee, W. Park, IEEE Photonics Techn. Lett. **20**(8), 641 (2008).
[8] M. Howerton, R. Moeller, A. Greenblatt, R. Krahenbuhl, IEEE Phot. Technol. Lett. **12**(7), 792 (2000).
[9] B. M. Rahman, S. Haxha, J. Lightwave Technol. **20**(10), 1856 (2002).
[10] S. Irmscher, R. Lewen, U. Eriksson, IEEE Phot. Technol. Lett. **14**(7), 923 (2002).
[11] Bahram Jalali, Phys. Stat. Sol. (a) **205**(2), 213 (2008).
[12] L. Liao, A. Liu, D. Rubin, J. Basak, Y. Chetrit, H. Nguyen, R. Cohen, N. Izhaky, M. Paniccia, Electron. Lett. **43**, 2253 (2007).
[13] L. Gu, W. Jiang, X. Chen, L. Wang, R. T. Chen, Appl. Phys. Lett. **90,** 071105 (2007).
[14] Jiu-Sheng Li, Opt. Laser Techn. **40**(6), 790 (2008).
[15] J. Brosi, C. Koos, L. C Andreani, M. Waldow, J. Leuthold, W. Freude, Opt. Express **16**, 4177 (2008).
[16] Wei Jiang, L. Gu, X. Chen, R.T. Chen, Solid State Electr. **51**(10), 1278 (2007).
[17] Y. Karla, R. K. Sinha, Opt. Quant. Electron. **37**, 889 (2005).
[18] P. Ma, F. Robin, H. Jäckel, Opt. Express **14**(16), 12794 (2006).
[19] R. D. Meade, A. M. Rappe, K. D. Brommer, J. D. Joannopoulos, J. Opt. Soc. Am. B **10**, 328 (1993).
[20] C. G. Bostan, R. M. de Ridder, J. Optoelectron. Adv. Mater. **4,** 921 (2002).
[21] F. Wen, S. David, X. Checoury, M. El Kurdi, P. Boucaud, Opt. Express **16** (16), 12278 (2008).
[22] B. R. Bennett, R. A. Soref, J. A. Alamo, IEEE J. of Quant. Electron. **26**, 113 (1990).
[23] M. Qiu, B. Jaskorzynska, M. Swillo, H. Benisty, Microwave Opt. Technol. Lett., **34**(5), 387 (2002).

*Corresponding author: gsksma@hol.gr